Effective Fokker-Planck equation: Path-integral formalism

T. G. Venkatesh and L. M. Patnaik
Microprocessor Applications Laboratory, Indian Institute of Science, Bangalore 560 012, India
(Received 14 December 1992; revised manuscript received 29 March 1993)

We derive an effective Fokker-Planck equation for a nonlinear non-Markovian stochastic process using path-integral formalism. The effective Fokker-Planck equation of our approximation scheme is local in state space and local in time, and its diffusion constant remains positive over the entire state space for all noise correlation time. The mean first passage time (MFPT) and the stationary probability density function (SPDF) for the case of a bistable potential driven by Ornstein-Uhlenbeck noise are computed. The MFPT is compared with that of earlier theories and with the numerical simulation results. The SPDF is compared with that of the results obtained through the matrix continued-fraction method. Interesting connections between the path-integral method and the functional-calculus approach to the colored noise problem are brought out.

PACS number(s): 05.40.+j, 02.50.−r, 05.70.Ln

I. INTRODUCTION

The focus of this paper is on one of the most debated problems in the field of stochastic physics—derivation of an effective Fokker-Planck equation (EFPE) for a colored-noise-driven stochastic differential equation [1]. The problem is to derive a Fokker-Planck type evolution equation for the probability density function of the process described by [2–4],

$$\dot{x}(t)=f(x(t))+g(x(t))\xi(t) . \tag{1}$$

In Eq. (1), $f(x(t))$ and $g(x(t))$ are in general nonlinear functions of $x(t)$, and $\xi(t)$ is the Ornstein-Uhlenbeck noise with mean value zero and with correlation function $\langle\xi(t)\xi(t')\rangle=(D/\tau)\exp(-|t-t'|/\tau)$, where D is the noise strength and τ is the noise correlation time. If the driving noise is Gaussian and δ-function correlated, the x process is Markovian, and we have a Fokker-Planck equation, i.e., an equation for the probability density of x which is local in time and space. If the noise has finite correlation time, x becomes a non-Markovian process and its evolution equation is in general nonlocal both in time and space [5]. This makes it difficult to get closed-form exact formulas for the statistical quantities of interest, especially the stationary probability density function (SPDF) and the mean first passage time (MFPT) of the x process. An exact formal evolution equation for the probability density function $P(x,t)$ of x process can be derived and it is a Kramer-Moyal series with the general term of the form [6]

$$D^{n/2}\tau^{n/2-1+m}\left[\frac{\partial}{\partial x}\right]^{n-k}P(x,t)$$

$$(n\geq 2,\ m\geq 0,\ 0\leq k\leq n-1) .$$

In order to derive an approximate Fokker-Planck type equation, Sancho *et al.* truncated and did a partial resummation of the exact formal non-Markovian evolution equation [7,8]. The resulting equation is called the best Fokker-Planck equation (BFPE). However, it has been criticized that it is not possible to identify all terms in the above-mentioned Kramer-Moyal series at any given order in the perturbation parameters and hence a truncation is not possible [1,9,10]. Hanggi *et al.* then proposed a state-independent diffusion constant, valid for small D [11]. However, it has been shown that the scheme of Hanggi *et al.* fails to reproduce the richness of the non-Markovian features induced by the color of the noise [12].

Before proceeding with the review of the literature further, we simplify Eq. (1) as follows. Without loss of generality for the one-dimensional case, we consider only the additive noise, i.e., we set $g(x(t))$ to be 1. We rewrite $f(x(t))$ as $-V'(x(t))$, i.e., negative gradient of the potential $V(x(t))$. With these simplifications we henceforth consider the equation

$$\dot{x}(t)=-V'(x(t))+\xi(t) . \tag{2}$$

By various methods, such as cumulant expansion [13,14], Furutsu-Novikov's technique [7,8], the projection operator method [15], and the functional-calculus method [16], one can derive equivalent formal evolution equations for $P(x,t)$ of Eq. (2). In the functional-calculus notation it reads [7] as

$$\frac{\partial P(x,t)}{\partial t}=-\frac{\partial}{\partial x}[-V'(x(t))P(x,t)]+\frac{\partial^2}{\partial x^2}D(x,t)P(x,t) , \tag{3}$$

with

$$D(x,t)P(x,t)=\iint D[\xi(t)]P[\xi(t)]\delta(x-x(t))\int_0^t dt'\frac{D}{\tau}e^{-|t-t'|/\tau}\exp\left[-\int_{t'}^t V''(x(u))du\right] . \tag{4}$$

In Eq. (4) $\iint$ represent the path integral over $\xi(t)$; $D[\xi(t)]$ is the measure for integration and $P[\xi(t)]$ is the probability of occurrence of $\xi(t)$ realization. By invoking the smallness of τ, Fox set $V''(x(u))=V''(x(t))$, $0\le u\le t$ [16]. This approximation converts the functional appearing inside the path integral to be independent of the paths, enabling a trivial path integration. Fox got at stationarity, $D_{\rm Fox}(x)=D/[1+\tau V''(x)]$. $D_{\rm Fox}(x)$ remains positive whenever $V''(x)$ is positive, but becomes negative in the region where $\tau\ge -V''(x)^{-1}$. For the well-discussed case of the bistable potential, $V(x)=x^4/4-x^2/2$, Fox's diffusion constant becomes negative for $\tau\ge 1$ in a region $-\sqrt{(\tau-1)/3\tau}\le x\le+\sqrt{(\tau-1)/3\tau}$. The BFPE also shares with Fox's EFPE the anomaly of the negative diffusion constant. However, in the case of BFPE Hannibal [17] has shown that by imposing a regularity condition at infinity, it is always possible to single out a non-negative, though nonanalytic solution for the diffusion constant.

Similarly, Tsironis and Grigolini showed that by removing the stationarity condition assumed by Fox one gets a time-dependent diffusion constant free from the negative diffusion constant anomaly for all x and τ. Tsironis and Grigolini call this approximation a local linearization theory (LLT) [18]. However for $\tau\ge 1$, the diffusion constant of LLT diverges to $+\infty$ as $t\to\infty$ in the region $|x|<\sqrt{(\tau-1)/3\tau}$. Hence the stationary probability density function of LLT vanishes for $|x|<\sqrt{(\tau-1)/3\tau}$, contradicting the matrix continued-fraction results [19]. Further, it has been shown that the MFPT computed by LLT coincides with that of Fox's EFPE in the region of validity of Fox's EFPE and both underestimate the MFPT computed by the matrix continued-fraction method [19]. Der has proposed a scheme based on operator cumulant approach which can be used to improve the LLT result systematically [20]. However, explicit comparison of the MFPT for the bistable system with the simulation results has not been carried out in Ref. [20]. The unified colored-noise approximation (UCNA) method of Jung and Hanggi proposes an EFPE with a positive definite diffusion constant arrived at by doing an adiabatic elimination in the Langevin equation (1) [21]. The UCNA scheme gives good results for the dynamics such as relaxation times and stationary correlation [22,23]. With this, we finish the brief discussion of the various EFPE's proposed so far. It is in this context we propose an EFPE in this paper. Our EFPE not only overcomes the negative diffusion constant anomaly but also gives good predictions for the MFPT and SPDF both in the small and large τ range.

The paper is organized as follows. In Sec. II we derive an EFPE using the path-integral method. Then we categorize the various approximation schemes proposed to solve nonlinear non-Markovian stochastic processes. In Sec. III, the MFPT for the case of the bistable potential driven by Ornstein-Uhlenbeck noise is computed, and the results are compared with that of earlier theories and with the numerical simulation results. The SPDF of x is computed in Sec. IV and is compared with that of matrix continued-fraction results. In Sec. V, we bring out the intimate connection between the functional-calculus method and the path-integral approach to the colored-noise problem. We then discuss some of the EFPE's proposed so far under the path-integral framework. Our results are finally summarized in Sec. VI.

II. AN EFPE: PATH-INTEGRAL METHOD

We derive an EFPE in this section, starting from Eqs. (3) and (4) using the path-integral formalism. We first rewrite Eq. (4) as

$$D(x,t)P(x,t)=\iint D[x(t)]P[x(t)]F[x(t)]\delta(x-x(t)) \tag{5}$$

thereby defining

$$F[x(t)]\equiv\int_0^t dt'\frac{D}{\tau}e^{-|t-t'|/\tau}\exp\left[-\int_{t'}^t V''(x(u))du\right] \tag{6}$$

and we have used the fact that $\iint D[\xi(t)]P[\xi(t)]=\iint D[x(t)]P[x(t)]$. The path probability $P[\xi(t)]$ for the Ornstein-Uhlenbeck process under consideration over the time interval $(0,t)$ is given by [24]

$$P[\xi(t)]=N\exp\left[\frac{-1}{4D}\int_0^t du[\xi(u)+\tau\dot{\xi}(u)]^2\right], \tag{7}$$

where N is a normalization constant. When $x(t)$ is related to $\xi(t)$ through Eq. (2), we have

$$P[x(t)]=N\exp\left[\frac{-S[x(t)]}{D}\right]J_\xi[x(t)], \tag{8}$$

with

$$S[x(t)]=\frac{1}{4}\int_0^t du\{(\dot{x}+V'(x)+\tau[\ddot{x}+\dot{x}V''(x)]\}^2, \tag{9}$$

where it is understood that the integrant in Eq. (9) is evaluated at the time u. $J_\xi[x(t)]$ is the Jacobian of transformation over the same time interval $(0,t)$ from the $\xi(t)$ realizations to the $x(t)$ realizations. Sticking to the midpoint discretization of the paths, $J_\xi[x(t)]$ is given by [24]

$$J_\xi[x(t)]=\exp\left[\frac{1}{2}\int_0^t[\tau^{-1}+V''(x(u))]du\right]. \tag{10}$$

We want an approximate formula for $D(x,t)$ from Eq. (5). In order to do the path integration in Eq. (5), we invoke the smallness of D, and apply the steepest-descent technique [24–27]. In the limit $D\to 0$, the major contribution to the path integral arises around the minimal action path (MAP), which minimizes the action $S[x(t)]$ in reaching $x(t)=x$ from $x(0)$. At stationarity, i.e., for $t\to\infty$, we take $x(0)$ to be the stable point to whose basin of attraction x belongs. In other words, we have assumed that the Brownian particle was at rest at the stable point (to whose basin of attraction x belongs) for a long time before an optimal fluctuation takes it to x [28,29]. Since $x(0)$ is a stable point, the MAP is time-translational invariant and so our assumption to let $t\to\infty$ becomes self-consistent. The condition minimizing the action is

$\delta S[x(t)]/\delta x(t)=0$, and for $S[x(t)]$ given by Eq. (9) the MAP is the solution of the nonlinear differential equation [24],

$$y^2-V'^2=\tau^2(2y^3y''+y^2y'^2+2y^3V'''-y^2V''^2) , \quad (11)$$

with suitable boundary conditions. In Eq. (11), y represent $\dot{x}$ and dashes represent derivatives with respect to x. In the limit $D\to 0$, we take the functional $F[x(t)]$ evaluated along the MAP out of the path integral, and perform the remaining path integral in Eq. (5), which simply yields $P(x,t)$. We therefore propose the effective diffusion constant in the small D limit as

$$D(x,t)=F_{\mathrm{MAP}}[x(t)] , \quad (12)$$

where $F_{\mathrm{MAP}}[x(t)]$ is the functional $F[x(t)]$ evaluated along the MAP (which minimizes the action involved in reaching x from the stable point to whose basin of attraction x belongs).

We now consider the widely discussed case of the bistable potential, $V(x)=x^4/4-x^2/2$ [30] and compute the diffusion constant given by Eq. (12). We rewrite Eq. (12) with Eq. (6) as

$$D(x,t)=F_{\mathrm{MAP}}[x(t)] = \int_0^t dt' \frac{D}{\tau} \exp\left[-\int_{t'}^t [\tau^{-1}+V''(x(u))]du\right] , \quad (13)$$

where $x(u)$ is given by the MAP. As mentioned already in the discussions following Eq. (10), we let $t\to\infty$ and take $x(t)=x$ and, $x(t'=0)=+1$ for $0\le x<\infty$, and $x(t'=0)=-1$ for $-\infty<x<0$. Let $z(t')$ and $w(u)$, represents the value of x along the MAP at the time t' and u, respectively. Let $y(z)$ and $y(w)$ represent the velocity variable y along the MAP, defined by Eq. (11) at the points z and w, respectively. Using the relation $y(z)=dz(t')/dt'$ and $y(w)=dw(u)/du$ we change the time variables t' and u into space variables z and w, respectively, and rewrite Eq. (13) as

$$D(x)=\int_{\pm 1}^x \frac{dz}{y(z)} \frac{D}{\tau} \exp\left[-\int_z^x [\tau^{-1}+V''(w)]\frac{dw}{y(w)}\right] , \quad (14)$$

where $y(z)$ and $y(w)$ are given by the solution of Eq. (11). Equation (14) gives the effective diffusion constant for the bistable potential driven by the Ornstein-Uhlenbeck noise. The similarity between the diffusion constant given by Eq. (14) and that given by LLT [18] is that both remain non-negative for all x and τ, the difference being that the diffusion constant of LLT is nonlocal in time (i.e., it involves a time integral), but local in space, whereas the $D(x)$ given by Eq. (14) is local in time, but nonlocal in space (i.e., it involves a spatial integral).

We now categorize the various approximation schemes that have been proposed to solve the nonlinear non-Markovian process and thereby see where our approximation scheme fits in the categorization. It is well known that the formal evolution equation of the nonlinear non-Markovian (NLNM) process is in general nonlocal in both time and space [5]. Whereas for a nonlinear Markov process we have a Fokker-Planck equation, for a linear non-Markov process we have a Fokker-Planck type equation which is local in space and time with a time-dependent diffusion constant. It can be seen that all attempts to approximately solve the NLNM process should either invoke a linearization and/or Markovianization scheme. Two ways of invoking linearization are as follows.

(1) Approximating the potential by a harmonic potential locally [18] or only at the turning points of the potential [9]. Because LLT does a local linearization but retains the non-Markovian nature of the x process, the resultant process is a linear non-Markovian process and hence LLT's EFPE has a time-dependent diffusion constant.

(2) Invoking the limit $D\to 0$, in which case the mean-square displacement of the Brownian particle within one noise correlation time is so less that we can assume the potential to be effectively harmonic over the state space explored by the Brownian particle within one noise correlation time. The small D assumption has been invoked under different formalisms, the path-integral method [25,24], the WKB approximation [31], and the steepest-descent method [32].

Schemes invoking Markovianization either take the limit $\tau\to 0$ [8,13,16] or $\tau\to\infty$ [18,33–36]; former being the off-white–noise case, while the latter makes the noise deterministic and hence the solution process x Markovian (Chap. III of [37]). Under the above categorization scheme, it can be identified that the approximation invoked to derive Eq. (14) is a Markovianization scheme, as it is assumed that the noise realizations are deterministic and always follow the MAP in the limit $D\to 0$. Note that in contrast to LLT, we do Markovianization but retain the full nonlinearity; hence the occurrence of many spatial derivatives of $V(x)$ in $D(x)$ [see Eqs. (14), (15), and (19)].

On comparing the LLT and our approach, with that of the BFPE and Fox's EFPE the reason for the negative diffusion constant anomaly becomes clear. The BFPE and the Fox's EFPE arrive at diffusion constants which are local in both time and space. Such diffusion constants show the negative diffusion constant anomaly when either the nonlinearity or non-Markovicity or their combination in some suitably defined sense crosses some threshold $[\tau\ge 1/V''(x)]$. On the other hand, schemes which advocate (a) a time-nonlocal diffusion constant (LLT) or (b) a space-nonlocal diffusion constant [Eqs. (3), and (14)] do not break down, though they become inaccurate outside their domain of validity. Also note that schemes that are currently popular, namely, the path-integral method [24] and the WKB approximation [31], also arrive at results which are nonlocal in space. The spatial integral manifests itself in the form of the occurrence of infinite spatial derivatives in their results.

On reconsidering the above-mentioned categorization scheme, it becomes apparent that a clear categorization of an approximation scheme as either a linearization or a

Markovianization scheme is spurious. In fact the path-integral technique invoking the $D \to 0$ limit [24] can also be viewed as a Markovianization scheme as it assumes the realizations of x to be deterministic (MAP). Also, usage of a linearization or Markovianization method may either give rise to a diffusion constant which is nonlocal in time or nonlocal in space as these two are interconvertible [see Eqs. (13) and (14)].

Finally it is also clear, that there is no superiority of one formalism compared to another (say, path integral compared to EFPE), but it is the approximation scheme one invokes that matters. That this is true, even for deriving the EFPE's, has been shown already [38].

III. MEAN FIRST PASSAGE TIME COMPUTATION FOR THE BISTABLE POTENTIAL

We compute in this section the MFPT for the bistable potential. For general τ, one has to solve Eq. (11) numerically to get the MAP, then compute the functional $F_{\mathrm{MAP}}[x(t)]=D(x)$, and substitute it in Eq. (16) for computing T_{top}. Rather, we use the approximate formula for the MAP in the asymptotic limits of small and large τ, and compute the diffusion constant and the MFPT in these limits only.

A. MFPT in the small τ limit

In the case of white noise ($\tau=0$), the MAP is given by $y=\pm V'(x)$ [24,28]. Note that for the initial point of the MAP, $x(t=0)=\pm 1$, the sign of y which is physically relevant ($y \le 0$ for $-\infty < x \le -1$, $0 \le x \le +1$ and $y \ge 0$ for $1 \le x < +\infty$, $-1 \le x \le 0$) coincides with the sign of $V'(x)$ for $(-\infty < x < +\infty)$. Therefore, we set $y=V'(x)$ in Eq. (14) in the white-noise limit. We have computed the diffusion constant given by Eq. (14), with the white-noise MAP for small values of τ. The resultant diffusion constant is found to be equal to D for all x, thus proving the correctness of Eq. (14) in the white-noise limit.

In the small-τ limit, an approximate solution for the MAP has been derived by Bray and co-workers [24] as follows. y is first expanded in powers of τ^2 and then substituted in Eq. (11). Then, on equating equal powers of τ in Eq. (11), Bray and co-workers get the small-τ MAP. The small-τ MAP starting at $x=-1$, and ending at an x lying in between -1 and 0 (called the uphill MAP) is given by [24]

$$y=V'+2\tau^2 V'^2 V'''+\tau^4(14V'^3V''^2+8V'^2V''^2V''' +10V'^3V''V''''+2V'^4V''''') . \tag{15}$$

Again using the coincidence of the sign of y along the MAP starting at ± 1, with that of $V'(x)$, it can be seen that Eq. (15) is the valid MAP for $-\infty < x < +\infty$ in the small-τ limit.

We have computed $D(x)$ by solving Eq. (14) numerically, with $y(z)$ and $y(w)$ given by Eq. (15). We computed $D(x)$ in the range $-3 \le x \le +3$ for various values of D and for $0.05 \le \tau \le 0.5$. The following were noticed with regard to the value of $D(x)$ computed using Eq. (14). (1) We found that $D(x=\pm 1/\sqrt{3}) \simeq D$, for all values of D and τ considered ($0.05 \le \tau \le 0.5$). (2) $D(x)$ is found to decrease as x moves towards the bottom of the positive or negative well, while $D(x)$ increases as x moves towards the barrier top. (3) Further, the rate at which $D(x)$ changes as x moves away from $x=\pm 1/\sqrt{3}$ increases with τ. (4) For $\tau < 0.5$, the rate at which $D(x)$ changes is always greater than the rate at which $D_{\mathrm{Fox}}(x)$ changes.

Note that if x is varied from $x=\pm 1$ to $x=0$, the relative change in our $D(x)$ [given by Eqs. (14) and (15)] is larger than the relative change in $D_{\mathrm{Fox}}(x)$. Larger relative change in our $D(x)$ compared to $D_{\mathrm{Fox}}(x)$ results in larger values of T_{top} computed using our $D(x)$, compared to the T_{top} of Fox's EFPE. For values of τ close to 1, $D_{\mathrm{Fox}}(x)$ diverges to infinity at the barrier top. Therefore comparison between the $D_{\mathrm{Fox}}(x)$ and our $D(x)$ is not carried out. The reason for getting $D(x) \simeq D$ at the inflection points ($x=\pm 1/\sqrt{3}$) of the potential is as follows. The potential becomes almost linear at $x=\pm 1/\sqrt{3}$; $V''(x)$ vanishes, but $V'''(x)$, and $V''''(x)$ do not. If we invoke a linearization scheme, the diffusion process becomes locally a linear non-Markovian process with the diffusion constant $D_{\mathrm{LLT}}(x)$, proposed by the LLT [18]. At stationarity, $D_{\mathrm{LLT}}(x)$ becomes $D_{\mathrm{Fox}}(x)$. As $D_{\mathrm{Fox}}(x)$ coincides with D for all τ at $x=\pm 1/\sqrt{3}$, we conclude that our approximation agrees with the approximation of LLT for small values of τ. However, as τ increases, the linearization procedure becomes invalid for the following reason. Let us suppose we analytically find $D(x)$ in Eq. (14). $D(x)$ will then have terms like $V'''(x)\tau^a$, $V''''(x)\tau^b$ and so on, where a, b, etc., are integers greater than 1. The $V'''(x)\tau^a$, $V''''(x)\tau^b$, and higher-order terms contribute non-negligible corrections to $D_{\mathrm{Fox}}(x)$ at $x=\pm 1/\sqrt{3}$. Hence the linearization scheme breaks down for large τ. Indeed for $\tau > 1$, $D(x=\pm 1/\sqrt{3})$ computed using Eqs. (14) and (19) is quite different from D. Also for $\tau > 1$, we find $D(x)$ to increase monotonically as x is changed from ± 1 to 0.

The MFPT T_{top}, for x to go from the bottom of one well to the barrier top of the bistable potential, is computed using Stratonovich's formula [27],

$$T_{\mathrm{top}}=\int_{-1}^{0}\frac{dx}{D(x)P_s(x)}\int_{-\infty}^{x}dy\,P_s(y) . \tag{16}$$

In order to do numerical integration we have truncated the range of the inner integral in Eq. (16) to $(-3 \le y \le x)$. The error introduced due to this truncation is very small. $P_s(x)$ in Eq. (16) is the stationary probability density function of x,

$$P_s(x)=\frac{N}{D(x)}\exp\left[\int_{-\infty}^{x}\frac{-V'(z)dz}{D(z)}\right] . \tag{17}$$

In Figs. 1, 2, and 3, we compare our results for T_{top}, and $T_{\mathrm{bot}}=2T_{\mathrm{top}}$ with the theoretical results of Fox [16], Klosek-Dygas, Matkowsky, and Schuss [31], and Bray and co-workers [24], and with the numerical simulation results of Mannella, Palleschi, and Grigolini [39]. As the MFPT of LLT coincides with that of Fox's EFPE in the

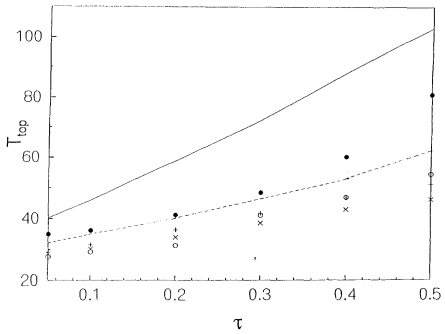

FIG. 1. T_{top} as a function of τ for $D=0.1$. The solid line represents T_{top} of Ref. [39]. The dashed line represents T_{top} of Ref. [19(a)]. The symbols are theoretical predictions; solid circles: Eqs. (16) with (14) and (15); pluses: path-integral method (Ref. [24]); open circles: Fox's EFPE (Ref. [16]); crosses: singular perturbation method (Ref. [31]).

small-τ regime [19], conclusions drawn on comparing our results with that of Fox's EFPE are also applicable for LLT. In Fig. 1, we have also plotted T_{top} computed using the matrix continued fraction (MCF) by Jung, Hanggi, and Marchesoni [19]. Note in Fig. 1 that the numerical simulation results [39] and the MCF results [19] differ considerably. From Fig. 1 we notice that our results agree with the MCF results better than other theories (only) for $\tau \lesssim 0.3$. However, we note in Figs. 1–3 that our results agree with the numerical simulation results better than the results of Fox's EFPE and that of singular perturbation method [31]. Surprisingly our results also agree with the simulation results better than the results of Bray and co-workers [24]. Note that Ref. [24] is also based on the path-integral method as is the case of our approach. Further Bray and co-workers use the MAP correct to $O(\tau^4)$ as we do, but avoid the Fokker-Planck approach for computing the MFPT. Note that the prefactor of the escape rate is computed in Ref. [24] by doing a Gaussian integration around the MAP, which is valid only in the small-D limit. Further, the escape rate is equated to the conditional probability

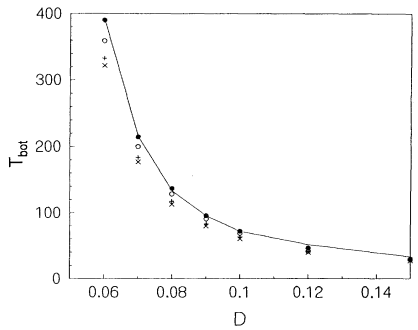

FIG. 2. T_{bot} as a function of D for $\tau=0.1$. The solid line represents T_{bot} of Ref. [39]. The symbols are theoretical predictions; solid circles: Eqs. (16) with (14) and (15); pluses: path-integral method (Ref. [24]); open circles: Fox's EFPE (Ref. [16]); crosses: singular perturbation method (Ref. [31]).

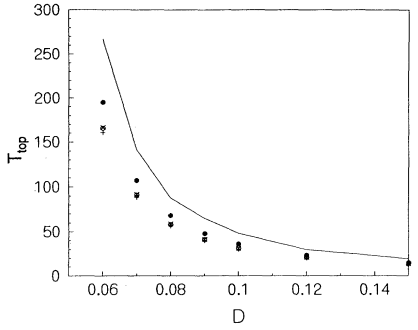

FIG. 3. T_{top} as a function of D for $\tau=0.1$. The solid line represent T_{top} of Ref. [39]. The symbols are theoretical predictions; solid circles: Eqs. (16) with (14) and (15); pluses: path-integral method (Ref. [24]); open circles: Fox's EFPE (Ref. [16]); crosses: singular perturbation method (Ref. [31]).

$P(+1,T/2|-1,-T/2)$ in the limit $T\to\infty$ (however, see Ref. [40] for the correct computation of the prefactor wherein the boundary terms in case of finite time intervals are taken into consideration), whereas in the case of Eq. (5), once F_{MAP} is taken out of the path integral in Eq. (5) (which is of course valid only in the limit $D\to 0$), the remaining path integral can be done exactly which simply yields $P(x,t)$. Also we use the exact formula for the T_{top}. Probably this factor might account for the better accuracy of our results compared to that of Ref. [24]. See in Fig. 2 the excellent agreement of our results (in general all theoretical predictions) with the simulation results for T_{bot}. But also notice in Fig. 3 a comparatively poor agreement between T_{top} of the theories with the numerical simulation results. All theories under discussion (except Ref. [31]) compute only T_{top} and predict T_{bot} as $2T_{top}$. However, the quantity of relevance at finite τ is $T_{sep}=\frac{1}{2}T_{bot}$, where T_{sep} is the MFPT to reach the separatrix curve of the (x,ξ) space from one of the metastable points [41]. In general $T_{bot}=\alpha T_{top}$, where $\alpha=2$ for $\tau=0$, $\alpha=1$ for $\tau\to\infty$ and $1\le\alpha\le 2$, at finite τ [41] (see also Fig. 4 of Ref. [34]). All theories underestimate T_{top} as shown in Fig. 3, but their $2T_{top}$, just happen to coincide exactly with T_{bot} almost compensating for the decrease in α for $\tau=0.1$.

B. MFPT in the large-τ limit

To get the MAP in the large τ limit, we closely follow Ref. [24]. First we rescale the time $t\to\tau t$, and therefore $y\to y/\tau$. With this scaling Eq. (11) becomes

$$\frac{y^2}{\tau^2}-V'^2=\tau^2\left[\frac{2y^3y''}{\tau^4}+\frac{y^2y'^2}{\tau^4}+\frac{2y^3V'''}{\tau^3}-\frac{y^2V''^2}{\tau^2}\right]. \tag{18}$$

Retaining only $O(\tau^0)$ terms in Eq. (18) we see that the physically relevant MAP is $y=V'/|V''|$ for $(-\infty<x<+\infty)$, derived already in Ref. [24]. However, this MAP is valid only for $\tau\to\infty$, and for finite τ it becomes invalid as $V''(x)$ vanishes at the inflection points of the potential. On retaining terms up to $O(\tau^{-1})$ in Eq.

(18) we have

$$\left[\frac{2V'''}{\tau}\right]y^3-V''^2y^2+V'^2=0\ . \tag{19}$$

Equation (19) has been solved for the MAP, and y is then rescaled as $y/\tau\rightarrow y$ to get back to the original time scale. Due to this rescaling the MFPT computed by us is already in the original time scale. The diffusion constant is computed using Eq. (14) with $y(z)$, and $y(w)$ from the solution of Eq. (19) for different values of D with $2\leq\tau\leq 10$ for $-3\leq x\leq 0$. The diffusion constant remains positive for all values of D and τ considered. We note that our EFPE results in a positive definite diffusion constant and a positive definite SPDF for all x and τ. This fact allows us to use Eq. (16) for computing the T_{top}, even in the large but finite-τ limit. The MFPT T_{top} is then computed as in the small-τ case using Eqs. (16) and (17). Figure 4, gives the comparison between the T_{top}, obtained as above with the numerical simulation results of Ref. [39]. We find that the T_{top} computed using Eq. (16) overestimates the simulation results; more is the overestimation in the limit $\tau/D\rightarrow\infty$. We now analyze the reason for the same. When we contract the two-dimensional Markovian dynamics of the (x,ξ) process onto a one-dimensional approximate dynamics of x, the separatrix of the two-dimensional MFPT problem does not get projected onto a single point on the x axis. Instead the separatrix gets projected onto the region $-1/\sqrt{3}\leq x\leq+1/\sqrt{3}$, with an unknown probability distribution. Only in the limit $D\rightarrow 0$ with either $\tau\rightarrow 0$ or $\tau\rightarrow\infty$, the probability distribution of the separatrix becomes peaked at a point on x axis ($x=0$, in the $\tau\rightarrow 0$, and at $x=\pm 1/\sqrt{3}$, in the $\tau\rightarrow\infty$ case). The distribution of the separatrix is unknown in the finite-τ limit. Computation of MFPT to reach a boundary with a probability distribution defined on it is not known. Hence the EFPE formalism is not valid for computing the MFPT at finite τ. Note that in the computation of T_{top}, the separatrix is assumed to be at the point $x=0$. Therefore, our T_{top} overestimates the numerical simulation results of Mannella, Palleschi, and Grigolini.

We further substantiate the distribution of the separatrix in the region $-1/\sqrt{3}\leq x\leq+1/\sqrt{3}$. Note that the separatrix gets projected onto the points $x=\pm 1/\sqrt{3}$ for $(\tau/D)\rightarrow\infty$. This fact inspired us to compute the MFPT of x from -1 to $-1/\sqrt{3}$, by setting to $-1/\sqrt{3}$ the upper limit of the integral over x in Eq. (16). We denote the MFPT from -1 to $-1/\sqrt{3}$ as $T_{-1/\sqrt{3}}$. Noting the nature of the distribution of the separatrix, we expect $T_{-1/\sqrt{3}}$ to underestimate the T_{top} of the simulation results at finite τ. We have computed $T_{-1/\sqrt{3}}$ for $2\leq\tau\leq 10$. $T_{-1/\sqrt{3}}$ is compared against the T_{top} of Mannella, Palleschi, and Grigolini [39] in Fig. 5.

Supporting our expectation, we notice in Fig. 5 that $T_{-1/\sqrt{3}}$ underestimates the T_{top} of the simulation results. We point out the similarity between the underestimation exhibited by our $T_{-1/\sqrt{3}}$, and the underestimation shown by $T_{-1/\sqrt{3}}$ of the UCNA scheme [42]. Notice in Figs. 10 and 11 that the SPDF in the $|x|\leq 1/\sqrt{3}$ region is vanishingly small. It is well known that the tails of the SPDF are the major contributor to the MFPT. Total negligence of the region $-1/\sqrt{3}\leq x\leq 0$, while computing $T_{-1/\sqrt{3}}$ by us, and by the UCNA scheme, has resulted in the underestimation of the MFPT by us and by the UCNA scheme on comparing both with the simulation results.

Notice that computation of $T_{-1/\sqrt{3}}$ is analogous to the assumption made by the fluctuating potential theory (FPT) for computing T_{bot} [18], the reason being the FPT theory assumes that the transition to the other well is immediate once x reaches $\pm 1/\sqrt{3}$. Also notice that both T_{bot} of the FPT and $T_{-1/\sqrt{3}}$ of our EFPE formalism underestimate T_{bot} of the simulation results, at finite τ. The following modifications have been made on the FPT to overcome the underestimation of T_{bot} by the FPT at finite τ, (a) by de la Rubia *et al.* [33], (b) by Ramirez-Piscina *et al.* [34], and (c) by us [35,36]. Recall that the total negligence of the region $-1/\sqrt{3}\leq x\leq 0$ while computing $T_{-1/\sqrt{3}}$ is responsible for the underestimation exhibited by $T_{-1/\sqrt{3}}$. Therefore the contributions to the MFPT, by the SPDF in the region $-1/\sqrt{3}\leq x\leq 0$ under

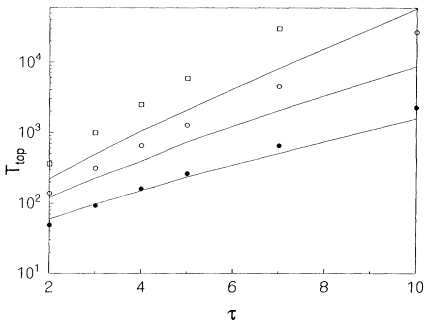

FIG. 4. T_{top} as a function of τ for various D. Solid lines are results of Ref. [39]. From top to bottom lines represent $D=0.15$, $D=0.2$, and $D=0.3$. The symbols are results of Eqs. (16) with (14) and (19); squares ($D=0.15$), open circles ($D=0.2$), and solid circles ($D=0.3$).

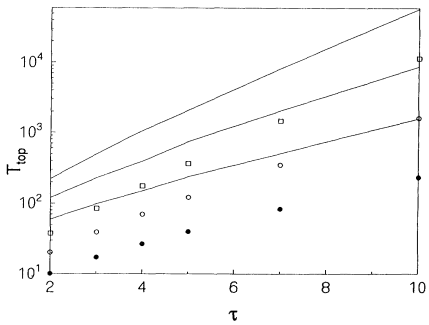

FIG. 5. $T_{-1/\sqrt{3}}$ of our results compared with T_{top} of Ref. [39] for various τ and D. Solid lines are T_{top} of Ref. [39]. From top to bottom solid lines represent $D=0.15$, $D=0.2$, and $D=0.3$. Symbols are $T_{-1/\sqrt{3}}$ of our results [using Eqs. (14) and (19)]; squares ($D=0.15$), open circles: ($D=0.2$), and solid circles ($D=0.3$).

the EFPE formalism, is analogous to the corrections proposed to the FPT.

Using the above-mentioned analogy between the EFPE formalism and the FPT, we analyze the separatrix issue. We notice that the FPT becomes valid in the region $-\sqrt{(\tau-1)/3\tau} \le x \le 0$ [35]. Hence at finite τ, we can assume the transition to take place once x reaches $-\sqrt{(\tau-1)/3\tau}$. Therefore we are led to believe that the MFPT from -1 to $-\sqrt{(\tau-1)/3\tau}$ might capture the effective projection of the separatrix. Also note that one can safely compute the MFPT from -1 to $-\sqrt{(\tau-1)/3\tau}$, even by the UCNA scheme, and by the Fox's EFPE method. We have computed T_{top} using Eq. (16) with this modification. Though there is a slight improvement in the coincidence with the numerical simulation results, the underestimation persists. Probably in the limit $D \to 0$, one can expect the MFPT from -1 to $-\sqrt{(\tau-1)/3\tau}$ to coincide with T_{bot}. We thus conclude that it is not easy (possible) to find out an effective point of projection of the separatrix curve onto the x axis and use it in the EFPE formalism to compute MFPT.

IV. THE STATIONARY PROBABILITY DENSITY FUNCTION

The SPDF given by Eq. (17) has been computed and it is shown in Figs. 6 and 7 for $\tau \le 0.5$. The behavior of the SPDF with a change in D or τ is in qualitative agreement with the conclusions drawn from the analog simulation [43] and from the MCF method [10]. In Fig. 8 we have compared the SPDF for $\tau=0.2$ and 0.4 with the MCF results of Ref. [3]. While plotting Fig. 8, we have adjusted the peak value of our SPDF to coincide with the SPDF curve of the MCF result. Figure 8 shows that our SPDF coincides well with the MCF results (but for the normalization constant). A similar close coincide with the SPDF of the MCF result is also exhibited by the UCNA scheme [3]. Figure 9 shows the SPDF for $2 \le \tau \le 10$ with $D=0.1$ in the vicinity of the bottom of the positive well. For large τ, the SPDF is highly peaked and is concentrated over a very narrow region around the stable points ± 1. The SPDF is nonzero, but becomes vanishingly small

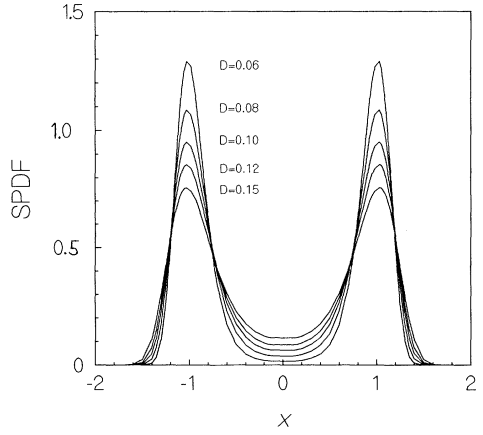

FIG. 6. The SPDF computed using Eq. (17) for various D at $\tau=0.1$.

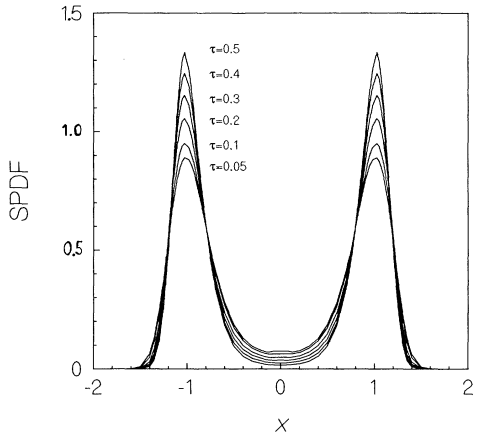

FIG. 7. The SPDF computed using Eq. (17) for various τ at $D=0.1$.

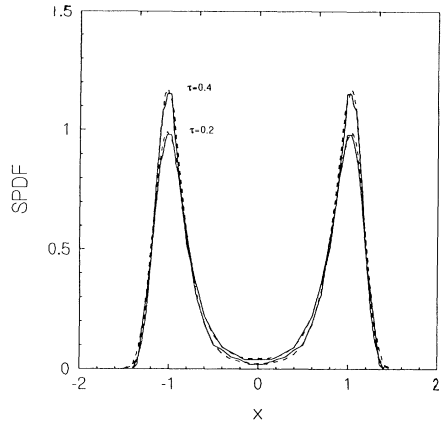

FIG. 8. The SPDF of our results computed using Eq. (17) (dashed lines) compared with the MCF results of Ref. [3] (solid lines) for $\tau=0.2$, 0.4, with $D=0.1$.

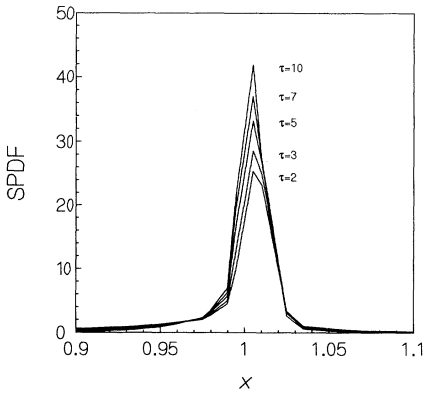

FIG. 9. The SPDF computed using Eq. (17) for various τ at $D=0.1$. The SPDF is plotted only in the vicinity of the bottom of the positive well.

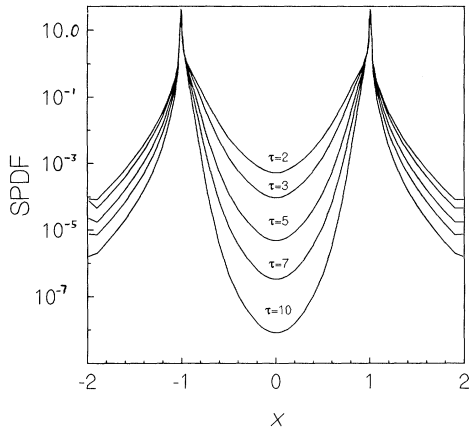

FIG. 10. The SPDF computed using Eq. (17) for various τ at $D=0.1$ plotted in the logarithmic scale.

with an increase in τ, at the barrier top. This is shown in Fig. 10.

The above-mentioned behavior of the one-dimensional SPDF of the x process is closely related to the analog simulation results of the two-dimensional SPDF of the (x,ξ) process [44,45]. The two-dimensional SPDF of the (x,ξ) process shows a complex topological change with an increase in τ. It has been pointed out that the topological changes induced by the color of the noise might have some effect on the choice of the integration path used in Sec. II [46].

In Fig. 11 the SPDF computed by us is compared with the SPDF obtained through the MCF method [19]. We point out that for large τ the value of the SPDF at the barrier top (and also at the bottom of the wells) is highly sensitive to the exactness of the theoretical and the numerical computation employed in arriving it. Due to this factor we could only get a fair agreement between our SPDF and the exact SPDF of the MCF method. In contrast to the conclusion drawn in Ref. [24] (but in agreement with the MCF results [19]) we do not see any plateau in the SPDF [and therefore in the action, $-D\ln P_s(x)$] for large τ, around $x=0$.

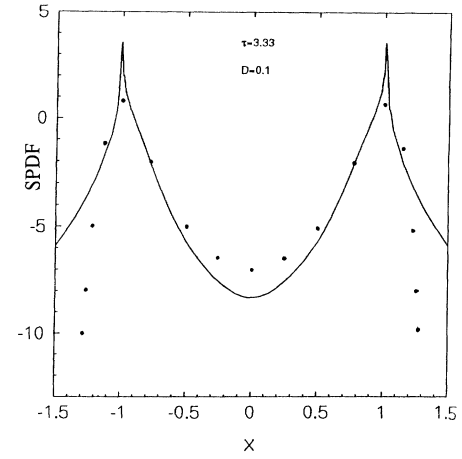

FIG. 11. Natural logarithm of SPDF computed using Eq. (17) (solid line) for $\tau=3.33$ and $D=0.1$ is compared against the MCF results of Ref. [19(a)] (solid circles).

V. RELATION BETWEEN THE FUNCTIONAL-CALCULUS FORMALISM AND THE PATH-INTEGRAL APPROACH

It has been pointed out that there is an intimate connection between the functional-calculus formalism and the path-integral method [16]. We substantiate this statement in this section and thereby analyze the various EFPE's under the path-integral framework. First we show that the Jacobian of transformation from the x realizations to the corresponding ξ realizations connected through Eq. (1) can be represented in terms of the response function, $\delta x(t)/\delta\xi(t')$.

Consider Eq. (1). Let $x(t)$ and $\xi(t)$ represent the values of x and ξ at the time t, and let $x[t]$ and $\xi[t]$ represent the entire realization of x and ξ over the time interval $(-\infty<t<+\infty)$. The physical interpretation of the Jacobian of transformation goes like this [47]. Every noise realization on the interval $(-\infty<t<\infty)$ gets mapped onto a unique realization of x through the relation defined by Eq. (1). Consider an infinitesimally small tube enclosing a noise realization $\xi[t]$. All noise realizations within this tube get mapped onto x realizations which are close by and form another tube in the space of x. The Jacobian $\delta x[t]/\delta\xi[t]$ is then defined as the ratio of the volume of the tube in the x space to the volume of the tube in the ξ space enclosing the noise realization $\xi[t]$, in the limit the volume of both the tubes tend to zero. In other words, Jacobian is the derivative of the x realization, $x[t]$ with respect to the noise realization $\xi[t]$. The derivative of $x[t]$ with respect to $\xi[t]$ can be defined as the total change in $x[t]$ [i.e., the sum of changes at $x(t)$; $-\infty<t<\infty$] due to infinitesimal unit perturbations at all points in the $\xi[t]$. Symbolically we then write the Jacobian as

$$\frac{\delta x[t]}{\delta\xi[t]}=\lim_{i\to\infty}\int_{-\infty}^{\infty}ds\frac{\delta x(s)}{\delta\xi(t_{-i})\cdots\delta\xi(t_1)\delta\xi(t_2)\cdots\delta\xi(t_i)} \tag{20}$$

which can be written in a compact notation as

$$\frac{\delta x[t]}{\delta\xi[t]}=\int_{-\infty}^{\infty}ds\prod_{-\infty}^{\infty}du\frac{\delta x(s)}{\delta\xi(u)}\ , \tag{21}$$

where $\delta x(s)/\delta\xi(u)$ is the functional derivative of the functional $x(s)$ with respect to $\xi(u)$, which is more commonly called the response function. By definition, we have got Eq. (21) relating the Jacobian and the response function. Instead the Jacobian is usually derived by discretizing the x and ξ paths, and writing the Jacobian as the determinant value of an infinite-dimensional matrix [26,27,48]. By taking the continuum limit of this matrix, one can arrive at Eq. (21). We prove Eq. (21), rather, by deriving the Jacobian from the response function. Our derivation is somewhat analogous to the method outlined in Ref. [48].

The response function $\delta x(s)/\delta\xi(u)$ for Eq. (1) has been

derived to be [3,7,8]

$$\frac{\delta x(s)}{\delta \xi(u)} = g(x(u))\Theta(s-u)\exp\left[\int_u^s dv\{f'(x(v))+g'(x(v))\xi(v)\}\right] . \tag{22}$$

Here Θ represents the unit-step function; $\Theta(t)=0$ for $t<0$ and $\Theta(t)=1$ for $t\geq 0$. Substituting Eq. (22) into Eq. (21), we have

$$\frac{\delta x[t]}{\delta \xi[t]} = \int_{-\infty}^{\infty} ds \prod_{-\infty}^{\infty} du\, g(x(u))\Theta(s-u)\exp\left[\int_u^s dv\{f'(x(v))+g'(x(v))\xi(v)\}\right] . \tag{23}$$

Noting that $\Theta(s-u)=0$, for $s<u$, and due to the presence of $\prod_{-\infty}^{\infty} du$, we find that the nonzero contribution to the integral over s, in Eq. (23) comes only for $s=+\infty$. With this simplification we have

$$\frac{\delta x[t]}{\delta \xi[t]} = \prod_{-\infty}^{\infty} du\, g(x(u))\exp\left[\int_u^{\infty} dv\{f'(x(v))+g'(x(v))\xi(v)\}\right] . \tag{24}$$

Splitting the product in Eq. (24) into a product over $g(x(u))$ multiplied by the product over $\exp[\cdots]$, and using the relation $\prod = \exp[\int]\ln$, we have

$$\frac{\delta x[t]}{\delta \xi[t]} = \exp\left[\int_{-\infty}^{\infty} du \ln|g(x(u))|\right]\left[\exp\int_{-\infty}^{\infty} du \ln\right]\exp\left[\int_u^{\infty} dv\{f'(x(v))+g'(x(v))\xi(v)\}\right] . \tag{25}$$

Simplifying, we have

$$\frac{\delta x[t]}{\delta \xi[t]} = \exp\left[\int_{-\infty}^{\infty} du \ln|g(x(u))|\right]\exp\left[\int_{-\infty}^{\infty} du \int_u^{\infty} dv\{f'(x(v))+g'(x(v))\xi(v)\}\right] , \tag{26}$$

which on further simplification becomes

$$\frac{\delta x[t]}{\delta \xi[t]} = \exp\left[\int_{-\infty}^{\infty} du \ln|g(x(u))|\right]\exp\left[\frac{1}{2}\int_{-\infty}^{\infty} dv\{f'(x(v))+g'(x(v))\xi(v)\}\right] . \tag{27}$$

Equation (27) coincides with the Jacobian derived in Ref. [26].

Further, we show that the formal effective diffusion function given by Eq. (5) can be written in terms of $J_{\xi}[x(t)]$, the Jacobian of transformation from the $\xi(t)$ realizations to the $x(t)$ realizations. Let $J_{\xi}[x,(t',t)]$ be the Jacobian of transformation from $\xi(t)$ to $x(t)$ over the time interval (t',t). We now write Eq. (5), with $F[x(t)]$, given in the form of Eq. (13) as

$$D(x,t)P(x,t) = \iint D[x(t)]P[x(t)]\int_0^t dt' \frac{D}{\tau} J_{\xi}[x,(t',t)]^{-2}\delta(x(t)-x) . \tag{28}$$

The representation of the $D(x,t)$, in terms of the Jacobian of transformation, gives us more insight into the negative diffusion phenomenon. We discuss this in the following. From Eq. (28) we see that if more probability is assigned to a x realization, for which the Jacobian is vanishingly small, the diffusion constant will tend to infinity. With this in mind let us analyze the diffusion constant proposed by Fox. $D_{\text{Fox}}(x)$ can be got by evaluating $F[x(t)]$ [given by Eq. (6)] using $x(u)=x(t)$, $0\leq u\leq t$. Therefore, from Eq. (12) we see that the assumption underlying Fox's approximation is that the most probable realization among the x realizations reaching the point x is $x(u)=x(t)$, $0\leq u\leq t$. If and only if x is a stable point, the noise realization corresponding to the x realization $x(u)=x(t)=x$, $0\leq u\leq t$, is $\xi(u)=0$, $0\leq u\leq t$, and hence both x and ξ realizations become most probable, making $D_{\text{Fox}}(x)$ exact. If x is not a stable point, $D_{\text{Fox}}(x)$ becomes inaccurate. In particular, if x is in the region where $[\tau^{-1}+V''(x)]<0$, the Jacobian [Eq. (10)], tends to zero as $t\to\infty$ for $x(u)=x(t)=x$, $0\leq u\leq t$, and so $D_{\text{Fox}}(x)$ tends to infinity in these region. Without letting $t\to\infty$, one gets the approximation of LLT.

The fact that Fox's approximation becomes exact when x is a stable point is the one responsible for the $D_{\text{Fox}}(x)$ to become exact for $\tau\to\infty$ [49]. In the case of large τ, x is always found in the instantaneous potential minima. Further, the minima itself changes in a time of $O(\tau)$. Hence the assumption $x(u)=x(t)$, $0\leq t'\leq t$ of Fox becomes valid in Eqs. (5) and (6) for $t\leq t'\leq t-\tau$, which is the majority contributor for $D_{\text{Fox}}(x)$.

Let us now analyze the effective diffusion constant of the BFPE. BFPE proposes the diffusion constant correct to $O(D)$ to be [8,13]

$$D_{\text{BFPE}}(x) = D\frac{f(x)}{g(x)}\left[1+\tau f(x)\frac{d}{dx}\right]^{-1}\frac{g(x)}{f(x)} . \tag{29}$$

In Ref. [38] it has been shown that $D_{\text{BFPE}}(x)$ can be derived from Eq. (5) by considering only the deterministic path $\dot{x}(t)=f(x(t))$, with $x(t)=x$, and with $x(0)=x_0$, where x_0 is the stable point to whose basin of attraction x belongs. In the light of the path-integral approach to EFPE, it can be easily seen that Ref. [38] indeed shows that if the MAP is taken as the deterministic path, $\dot{x}(t)=f(x(t))$ with $x(0)=x_0$ and $x(t)=x$, then one arrives at $D_{\text{BFPE}}(x)$. But note that the path $\dot{x}(t)=f(x(t))$ with $x(0)=x_0$ and $x(t)=x$ is not a valid deterministic path because $x(t)$ cannot leave its initial stable position

x_0 due to deterministic force. Instead if we consider the path $\dot{x}(t)=-f(x(t))$, with $x(0)=x_0$ and $x(t)=x$, following Ref. [38], it can be shown that this path also leads to $D_{\mathrm{BFPE}}(x)$ with the same positivity requirement on the function $h(x,\tau)$ given by Eq. (2.20) of Ref. [38]. In fact the path $\dot{x}(t)=-f(x(t))$, is the so-called antideterministic path or MAP of x driven by white noise [28,40]. For the white noise $\eta(t)$ driving additively Eq. (1), the MAP is $\eta(t)=-2f(x(t))$ which leads to the MAP of x as $\dot{x}(t)=-f(x(t))$. Therefore, it becomes clear that BFPE proposes for all τ the diffusion constant given by Eq. (12) with the MAP of x driven by the white noise itself.

It can be seen that the action involved in reaching the point $x=0$ from $x=\pm 1$ is least only if $\dot{x}(t)=-f(x(t))$, which means that the noise realization should be $-2f(x(t))$. Note that the white noise can take independent values at distinct time instants, however, close the time instants may be. Therefore, whatever may be the nature of the potential, the MAP of the white noise is always $-2f(x(t))$. Hence the action and the MFPT is minimal in the white-noise case. However, if the noise has finite correlation time, their trajectories are not as flexible as the white-noise trajectories so as to mold themselves to the nature of the potential. Hence the path $-2f(x(t))$ no more corresponds to the least action for a colored noise. This is reflected by the presence of the term $\tau\dot{\xi}(t)$ in the action. Especially in the region where the inverse of the time scale of evolution of $\xi(t)$ [which is of $O(\tau^{-1})$], is less than $f'(x(t))$ [which is proportional to the derivative of the path $-2f(x(t))$], the usage of white-noise MAP for computing the effective diffusion constant at finite τ proposed by the BFPE breaks down.

VI. CONCLUSIONS

We will summarize the main points of this paper. An EFPE for a nonlinear non-Markovian stochastic process is derived using the path-integral method. The proposed EFPE is local in space and time, and its diffusion constant remains positive for all τ at all x. Both LLT and our approach propose non-negative SPDF of x for all τ, but this is achieved only at the cost of increase in the overhead involved in computing the diffusion constant. The intrinsic complexity associated with the nonlinear non-Markovian problem demands this overhead, if one wants an EFPE which does not break down. However, in contrast with the LLT, but in agreement with the MCF results [19], the SPDF computed through our scheme does not vanish at the barrier top for large τ. An attempt is made to categorize various approaches proposed to solve the nonlinear non-Markovian process. The MFPT for the case of bistable potential driven by Ornstein-Uhlenbeck noise is computed and compared with that of earlier theories, MCF, and numerical simulation results. It is found that all theories underestimate T_{top} in the small but finite-τ regime. In the case of large but finite τ, the proposed EFPE gives a good estimate for the SPDF. We show that the EFPE formalism is invalid for computing the MFPT at finite τ as the separatrix for the one-dimensional MFPT problem is unknown for finite τ. Interesting relations between the path-integral formalism and the functional-calculus approach are brought out. The Jacobian of transformation from the x realization to the noise realization is derived in terms of the response function. The Fox's EFPE and the BFPE are analyzed under the path-integral framework.

[1] P. Hanggi, F. Marchesoni, and P. Grigolini, Z. Phys. B **56**, 333 (1984).

[2] Katja Lindenberg, Bruce J. West, and Jaume Masoliver, in *Noise in Nonlinear Dynamical Systems,* edited by F. Moss and P. V. E. McClintock (Cambridge Univ. Press, Cambridge, 1989), Vol. 1.

[3] P. Hanggi, in *Noise in Nonlinear Dynamical Systems* (Ref. [2]).

[4] J. M. Sancho and M. San Miguel, in *Noise in Nonlinear Dynamical Systems* (Ref. [2]).

[5] H. Grabert, P. Hanggi, and P. Talkner, J. Stat. Phys. **22**, 537 (1980).

[6] N. G. van Kampen, J. Stat. Phys. **54**, 1289 (1989).

[7] P. Hanggi, Z. Phys. B **31**, 407 (1978).

[8] J. M. Sancho, M. San Miguel, S. Katz, and J. D. Gunton, Phys. Rev. A **26**, 1589 (1982).

[9] F. Marchesoni, Phys. Rev. A **36**, 4050 (1987).

[10] (a) Th. Leiber, F. Marchesoni, and H. Risken, Phys. Rev. A **38**, 983 (1988); (b) Th. Leiber, F. Marchesoni, and H. Risken, Phys. Rev. Lett. **59**, 1381 (1987).

[11] P. Hanggi, T. J. Mroczkowski, F. Moss, and P. V. E. McClintock, Phys. Rev. A **32**, 695 (1985).

[12] L. A. Lugiato and R. J. Horowicz, J. Opt. Soc. Am. B **2**, 971 (1985).

[13] K. Lindenberg, and B. J. West, Physica A **119**, 485 (1983); **128**, 25 (1984).

[14] N. G. van Kampen, Physica (Utrecht) **74**, 215 (1974); **74**, 239 (1974).

[15] P. Grigolini, Phys. Lett. A **119**, 157 (1986).

[16] R. F. Fox, Phys. Rev. A **33**, 467 (1986); **34**, 4525 (1986).

[17] L. Hannibal, Phys. Lett. A **145**, 220 (1990).

[18] G. Tsironis and P. Grigolini, Phys. Rev. Lett. **61**, 7 (1988); Phys. Rev. A **38**, 3749 (1988).

[19] (a) P. Jung, P. Hanggi, and F. Marchesoni, Phys. Rev. A **40**, 5447 (1989); (b) Th. Leiber, F. Marchesoni, and H. Risken, *ibid.* **40**, 6107 (1989).

[20] R. Der, Phys. Lett. A **135**, 430 (1989).

[21] P. Jung and P. Hanggi, Phys. Rev. A **35**, 4464 (1987).

[22] L. H'walisz, P. Jung, P. Hanggi, P. Talkner, and L. Schimansky-Geier, Z. Phys. B **77**, 471 (1989).

[23] P. Jung and P. Hanggi, J. Opt. Soc. Am. B **5**, 979 (1988).

[24] A. J. Bray, A. J. McKane, and T. J. Newman, Phys. Rev. A **41**, 657 (1990); A. J. McKane, H. C. Luckock, and A. J. Bray, *ibid.* **41**, 644 (1990); H. C. Luckock and A. J. McKane, *ibid.* **42**, 1982 (1990); K. M. Rattray and A. J. McKane, J. Phys. A **24**, 4375 (1991).

[25] J. F. Luciani and A. D. Verga, J. Stat. Phys. **50**, 567 (1988).

[26] P. Hanggi, Z. Phys. B **75**, 275 (1989).

[27] R. L. Stratonovich, in *Noise in Nonlinear Dynamical Systems* (Ref. [2]).

[28] M. I. Dykman, Phys. Rev. A **42**, 2020 (1990).

[29] A. Forster and A. S. Mikhailov, Phys. Lett. A **126**, 459 (1988).
[30] Katja Lindenberg, Bruce J. West, and George P. Tsironis, *Reviews of Solid State Science* (World Scientific, Singapore, 1989), Vol. 3, No. 2, p. 143.
[31] M. M. Klosek-Dygas, B. J. Matkowsky, and Z. Schuss, Phys. Rev. A **38**, 2605 (1988).
[32] Hu Gang and H. Haken, Phys. Rev. A **41**, 7078 (1990).
[33] F. J. de la Rubia, E. Peacock-Lopez, George P. Tsironis, K. Lindenberg, L. Ramirez-Piscina, and J. M. Sancho, Phys. Rev. A **38**, 3827 (1988).
[34] L. Ramirez-Piscina, J. M. Sancho, F. J. de la Rubia, Katja Lindenberg, and George P. Tsironis, Phys. Rev. A **40**, 2120 (1989).
[35] T. G. Venkatesh and L. M. Patnaik, Phys. Rev. A **46**, R7355 (1992).
[36] T. G. Venkatesh and L. M. Patnaik, Phys. Rev. E **47**, 1589 (1993).
[37] C. W. Gardiner, *Handbook of Stochastic Methods for Physics, Chemistry, and the Natural Sciences* (Springer, Berlin, 1983).
[38] Enrique Peacoak-Lopez, Bruce J. West, and Katja Lindenberg, Phys. Rev. A **37**, 3530 (1988).
[39] R. Mannella, V. Palleschi, and P. Grigolini, Phys. Rev. A **42**, 5946 (1990).
[40] Horacio S. Wio, P. Colet, M. San Miguel, L. Pesquera, and M. A. Rodriguez, Phys. Rev. A **40**, 7312 (1989).
[41] P. Hanggi, P. Jung, and P. Talkner, Phys. Rev. Lett. **60**, 2804 (1988).
[42] P. Hanggi, P. Jung, and F. Marchesoni, J. Stat. Phys. **54**, 1367 (1989).
[43] L. Fronzoni, P. Grigolini, P. Hanggi, F. Moss, R. Mannella, and P. V. E. McClintock, Phys. Rev. A **33**, 3320 (1986).
[44] F. Marchesoni and F. Moss, Phys. Lett. A **131**, 322 (1988).
[45] G. Debnath, F. Moss, Th. Leiber, H. Risken, and F. Marchesoni, Phys. Rev. A **42**, 703 (1990).
[46] A. J. Bray and A. J. McKane arrived at this conclusion.
[47] A. S. Mikhailov and A. Yu. Loskutov, *Foundations of Synergetics II, Complex Patterns* (Springer, Berlin, 1991).
[48] R. Phythian, J. Phys. A **10**, 777 (1977).
[49] P. Grigolini, L. A. Lugiato, R. Mannella, P. V. E. McClintock, M. Merri, and M. Pernigo, Phys. Rev. A **38**, 1966 (1988).